TISSUE ENGINEERING: Part A
Volume 16, Number 4, 2010

DOI: 10.1089/ten.tea.2009.0442

Self-Assembly of Aligned Tissue-Engineered Annulus Fibrosus and Intervertebral Disc Composite Via Collagen Gel Contraction

Robby D. Bowles, B.S.,[1] Rebecca M. Williams, Ph.D.,[1]
Warren R. Zipfel, Ph.D.,[1] and Lawrence J. Bonassar, Ph.D.[2]

Many cartilaginous tissues such as intervertebral disc (IVD) display a heterogeneous collagen microstructure that results in mechanical anisotropy. These structures are responsible for mechanical function of the tissue and regulate cellular interactions and metabolic responses of cells embedded within these tissues. Using collagen gels seeded with ovine annulus fibrosus cells, constructs of varying structure and heterogeneity were created to mimic the circumferential alignment of the IVD. Alignment was induced within gels by contracting annular gels around an inner boundary using both a polyethylene center and alginate center to create a composite engineered IVD. Collagen alignment and heterogeneity were measured using second harmonic generation microscopy. Decreasing initial collagen density from 2.5 mg/mL to 1 mg/mL produced greater contraction of constructs, resulting in gels that were 55% and 6.2% of the original area after culture, respectively. As a result, more alignment occurred in annular-shaped 1 mg/mL gels compared with 2.5 mg/mL gels ($p < 0.05$). This alignment was also produced in a composite-engineered IVD with alginate nucleus pulposus. The resulting collagen alignment could promote further aligned collagen development necessary for the creation of a mechanically functional tissue-engineered IVD.

Introduction

Lower back pain (LBP) is one of the leading causes of disability in the United States with estimated indirect and direct annual costs ranging from $20 to $100 billion.[1] LBP is frequently associated with diseased or injured intervertebral disc (IVD).[2–5] The IVD has two distinct regions, the annulus fibrosus (AF) and nucleus pulposus (NP), that are biochemically, mechanically, and cellularly distinct and work in concert to provide mechanical function.[6–9] The NP is primarily responsible for providing the IVD with its compressive properties, whereas the AF provides the shear and tensile properties and containment of the NP.[10] The NP extracellular matrix is unaligned and composed primarily of type II collagen and proteoglycans. In contrast, the AF is highly organized and predominantly composed of type I collagen and proteoglycans.[6,11–16] This highly organized aligned collagen fibril architecture provides the IVD with many of its complex anisotropic shear and tensile mechanical properties.[17] It is the complex architecture of the IVD that is responsible for providing mobility to the spine while handling the hoop, torsional, and bending stresses imposed upon it during motion of the spine.

Current treatments for degenerative disc disease include spinal body fusions, partial discectomies, NP replacements, and total disc replacements.[18] Spinal body fusions and partial discectomies focus on alleviating the symptoms of LBP, but do not focus on maintaining function of the spine and the IVD. Further, spinal body fusions often result in degeneration and damage to the adjacent disc levels due to the altered biomechanics.[19] Replacing degenerated nuclear material holds promise for treating IVD disease, but can only be applied when the AF tissue is healthy.

Synthetic total disc replacements are used to completely replace the diseased IVD tissue and maintain the function of motion segments.[20–23] However, the long-term performance of these implants and their effects on the adjacent disc levels are unknown. Further, wear and fatigue that likely will occur in synthetic discs present additional complications for clinical use. As a result, recent efforts have focused on using tissue engineering strategies that can replace diseased IVD tissue to treat LBP.

Efforts to develop a tissue-engineered IVD have focused largely on generating NP tissue, with fewer studies focusing on the AF.[24–28] The NP is an ideal target for tissue engineering due to the isotropic nature and gel-like structure. However,

[1]Department of Biomedical Engineering, Cornell University, Ithaca, New York.
[2]Department of Biomedical Engineering & Sibley School of Mechanical and Aerospace Engineering, Cornell University, Ithaca, New York.

because IVD disease and injury are often not limited to the NP, developing an implant that also focused on the AF is likely necessary for a variety of applications. A number of scaffolds have been suggested for AF tissue engineering, including porous silk scaffolds,[29] an alginate/chitosan hybrid,[30] demineralized bone matrix,[31] electrospun poly(ε-caprolactone) (PCL) fibers,[32,33] hyaluronic acid/nanofibrous scaffold,[34] collagen/glycosaminoglycan scaffolds,[35] and polyglycolic acid mesh.[36,37] Mizuno *et al*. developed a composite structure of both the AF and NP,[36,37] but these structures had limited collagen organization in the AF. To date, few studies have attempted to address the aligned and anisotropic nature of the AF: the first used electrospun nanofibrous scaffolds with aligned PCL fibers,[32,33] whereas the second used a wet-spinning and lyophilization technique to create an aligned alginate/chitosan scaffold.[30] In contrast, this work will attempt to create such collagen alignment using biological self-assembly that can be employed in an engineered composite IVD containing both AF and NP.

In efforts to engineer other types of tissue, aligned collagen fibril architectures have been generated by contracting collagen gels under a variety of boundary conditions.[38–40] Costa *et al*.[41] used this technique to create circumferentially aligned fibrils by imposing an annular outer boundary on contracting collagen gels seeded with human-dermal fibroblasts. The use of an inner mandrel has also been shown to produce aligned structures in tissue-engineered blood vessels.[42] The current study extends this work to create and regulate circumferential fibril alignment in tissue-engineered AF using cell-induced contraction of collagen gels around inner mandrels. Although the native AF has a multilamellar cross-ply organization of the collagen fibrils, the larger circumferential organization is responsible for resisting the hoop stresses experienced during compression. For this reason this study has focused on creating circumferential alignment utilizing AF cells. The specific objectives of this study were to examine the influence of boundary geometry and construct composition on the development of collagen architecture induced by AF-cell-driven gel contraction using second harmonic generation (SHG) and two-photon excited fluorescence (TPEF) microscopy[43–45] to image cell and collagen alignment. As a result, the purpose of this work was to demonstrate the feasibility of this technique and develop an understanding of the resulting collagen alignment that could be applied in future work to create mature engineered IVD.

Materials and Methods

Cell preparation

The cell preparation techniques were based on previously described techniques.[37] Sixteen IVDs were dissected out of the lumbar spine region of four adult skeletally mature (~14 month old) Finn/Dorset cross male sheep (Cornell University Sheep Program, Ithaca, NY) and washed in phosphate-buffered saline (PBS) (Dulbecco's PBS; Gibco BRL, Grand Island, NY). The AF region of the discs was separated from the NP and dissected into small pieces that were digested in 200 mL of 0.3% w/v collagenase type II (Cappel Worthington Biochemicals, Malvern, PA) at 37°C for 9 h. Digested tissue was filtered through a 100 μm nylon mesh (BD Biosciences, Bedford, MA) and centrifuged at 936 *g* for 7 min. The cells were washed three times in PBS, counted, and seeded at a density of 2500 cells/cm^2 in culture flasks with Ham's F-12 media (Gibco BRL) containing 10% fetal bovine serum (Gemini Bio Products, Sacramento, CA), ascorbic acid (25 μg/mL), penicillin (100 IU/mL), streptomycin (100 μg/mL), and amphotericin B (250 ng/mL). Cells were cultured to confluence at 37°C, 5% CO_2 atmosphere, normoxia, pH of 7.2, and 300 mOsm. After culture, cells were removed from T-150 flasks with 0.05% trypsin (Gibco). Cell viability and number were counted with a hemocytometer and trypan blue vital dye. Cells were then diluted to the appropriate concentrations and seeded in collagen gels.

Collagen solution preparation

Collagen type I was obtained from rat tails using established protocols (Pel-Freez Biologicals, Rogers, AZ).[46] Briefly, tendons were dissected from rat tails and transferred to a solution of dilute acetic acid (0.1%) at a volume of 80 mL/g of tendon at 4°C for 48 h. The solution was centrifuged at 9000 rpm, and the supernatant was transferred and centrifuged a second time to remove the unsolubilized collagen, blood, and muscle tissue. The solution was then subjected to the bicinchoninic acid (BCA) assay (Pierce, Rockford, IL) to determine the collagen concentration of the resulting solution. The stock solution was stored at 4°C until needed.

Collagen construct fabrication

Before producing gels, tissue culture plates were incubated with a 2% bovine serum albumin solution at 37°C for 1 hour to prevent construct adhesion to tissue culture plates upon gelation. The stock collagen solution was mixed with the appropriate volumes of 1 N NaOH, 1× PBS, and 10× PBS to return the pH to 7.0, maintain 300 mOsm, and produce the appropriate collagen concentrations for the study.[47] This solution was immediately mixed at a 1:1 ratio with the cell/media solution and pipetted into the appropriate tissue culture plate and allowed to gel for 30 min at 37°C. After the constructs had gelled, they were floated with 2 mL of the previously described media.

Collagen disk and annular constructs

A total of 70 collagen disk constructs were created by pipetting 1 mL of collagen–cell solution into a 24-well tissue culture plate and allowing it to gel. Collagen annular constructs were created by pipetting 1 mL of the collagen–cell solution into a 12-well tissue culture plate with a 1-cm-diameter porous polyethylene disk at the center to yield an annular-shaped collagen ring surrounding the polyethylene. The porous disk was selected to encourage gel to remain around disk when floated with media. Two groups were made for both construct shapes with final collagen concentrations of 2.5 mg/mL and 1 mg/mL and a final cell concentration of 1×10^6 cells/mL. The discs were floated with 1 mL of media for the disk constructs and 2 mL of media for annular constructs in each well to maintain similar degree of floating in wells during culture. Seven constructs per group were used for LIVE/DEAD cell viability assay (Invitrogen, Carlsbad, CA) immediately after construction. In addition, constructs were cultured for 3 days and allowed to contract freely with 7 constructs per group being harvested at 0, 1, 2, and 3 days. At each time point, constructs were digitally photographed to quantify construct area, and then fixed with

phosphate-buffered formalin for 48 h, with sections of each sample being utilized for SHG microscopy analysis of collagen fibril orientation and histology.

Composite discs

Alginate hydrogel NP was produced by mixing 3% (w/v) alginate seeded with 25×10^6 cells/mL with 2% $CaSO_4$ at 2:1 ratio and injected between glass plates to produce 2-mm-thick alginate sheet. 1.5 mm biopsy punch was shaped into NP shape dimensions obtained from rat lumbar discs and NP was punched out of sheet. Alginate NP was subsequently placed at the center of a 24-well plate and 0.405 mL of 2 mg/mL collagen solution was pipetted around alginate NP to produce 2-mm-thick collagen ring surrounding 2-mm-thick NP. A total of 21 composite discs were made and 7 constructs were used for LIVE/DEAD cell viability assay (Invitrogen) immediately after construction. Gels were then floated with 1 mL of media and allowed to culture for 0 and 2 weeks with seven discs being harvested at each time point and processed in similar manner to annular and disk constructs.

Digital imaging

All constructs were imaged with a digital camera (Canon Powershot G5) and quantitatively analyzed for surface area using the Image J software (NIH, Bethesda, MD) immediately after harvest on 0, 1, 2, and 3 days.

SHG and TPEF microscopy

Procedures of simultaneous SHG microscopy of collagen type I fibrils and TPEF microscopy of cells were based on those described previously.[43,45] SHG and TPEF images were obtained using a custom-built multi-photon microscope with a Ti:Sapphire mode-locked laser providing 100 fs pulses at 80 MHz tuned to a wavelength of 780 nm. Images were acquired using a BioRad (Hercules, CA) 1024 laser scanner coupled to an Olympus (Center Valley, PA) 1X-70 inverted microscope. Incident light was focused on the sample using either a 40× or a 20× objective. Samples were loaded onto the microscope so that fibrils aligned in the circumferential direction of the constructs were in the 90° direction according to a specified coordinate system (Fig. 1). Two-photon fluorescence and back-propagating second harmonic signals were collected and separated by a dichroic filter into two photomultiplier tubes (PMTs). One PMT collected the epi-SHG at 360–410 nm produced by the collagen type I fibrils, and the other PMT collected TPEF signal at 420–500 nm produced by the cells (primarily NADH). For both annular and disk constructs, SHG images were obtained to study the collagen fibril orientation throughout contraction. Z-series were collected with a 20×/0.7 NA water immersion objective to a depth of 80 μm (9 images at 10 μm intervals) at the outer, middle, and inner regions of the gels. The images were obtained for four samples for each time point and construct type. Images were also taken at higher resolution with an Olympus 40×/1.3 NA oil objective to observe fibril and cellular interactions.

Image analysis

Collagen fibril orientation was calculated from SHG images with a custom MATLAB code based on a previously described technique.[48] This technique has been applied to scanning electron microscopy, and histological and confocal images, and is applied to SHG images in the present study.[49–52] The algorithm relies on the fast fourier transform (FFT) of the SHG images (Fig. 2A). The program summed the intensity of the FFT along lines at 5° increments from 0 to 180° (Fig. 2B) via the coordinate system described (Fig. 1). The angular distribution of summed intensities was calculated, representing the relative orientation of the fibrils within the image (Fig. 2C). From this histogram, the mode was calculated, which represents the angle of maximum alignment, and using Equation 1 an alignment index (AI) was calculated.

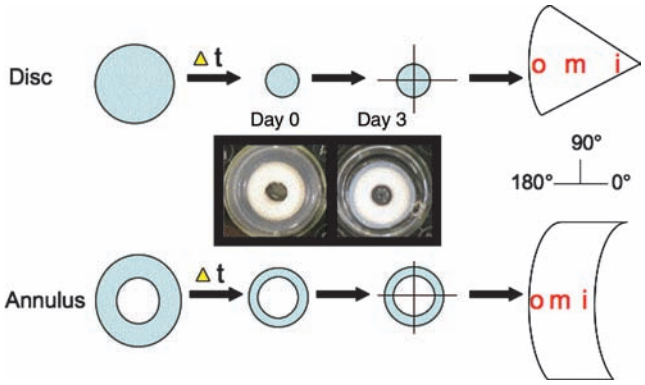

FIG. 1. Overview of gel culture and imaging methods. Annulus and disk gels were contracted over 3 days before being segmented for imaging. Images were obtained from the outer (o), middle (m), and inner (i) regions of each gel, as defined here. Coordinates were defined in reference to the imaged gel segments. Color images available online at www.liebertonline.com/ten.

$$AI = \frac{\int_{\theta_m-20^\circ}^{\theta_m+20^\circ} I\partial\theta}{(40^\circ/180^\circ)\times\int_{0^\circ}^{180^\circ} I\partial\theta} \quad (1)$$

AI ranges from 1 (unaligned) to 4.5 (complete alignment of fibers). Together, the AI provides the degree of alignment observed, whereas the mode angle provides the direction of alignment.

Histological analysis

One sample at each time point was fixed for 24 h with 10% phosphate-buffered formalin. The specimens were embedded within paraffin, and serial sections of 5 μm were cut and stained with hematoxylin and eosin for comparison to SHG and TPEF images.

Statistical analysis

All statistical analysis was performed using three-factor analysis of variance and Bonferroni *post hoc* test. The AI parameter was tested for the effect of time in culture (0, 1, 2, and 3 days), region of gel (outside, middle, and inside), and density of gel (1 mg/mL and 2.5 mg/mL).

Results

Contraction

Macro scale. The disk and annular constructs followed a similar contraction profile (Fig. 3). The 2.5 mg/mL disks

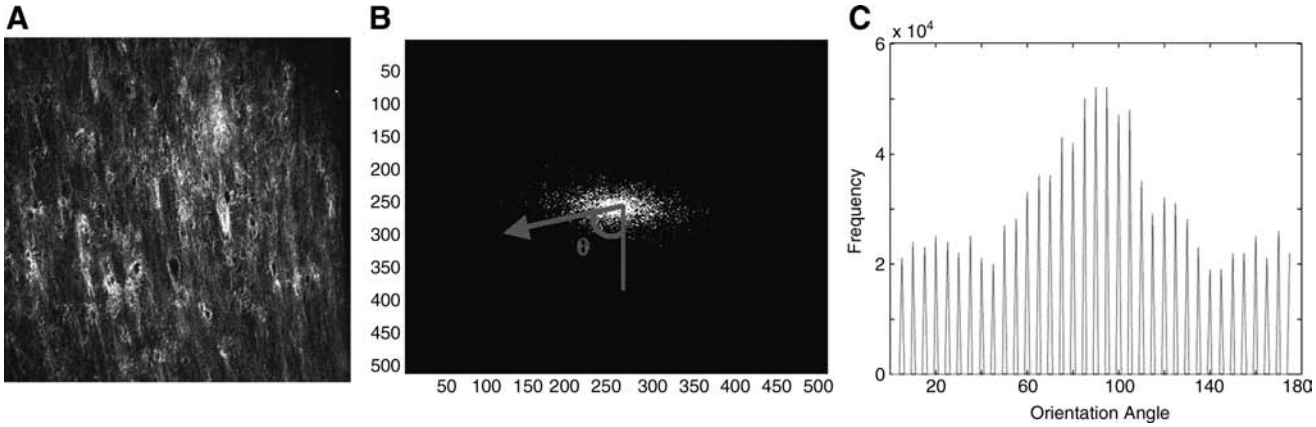

FIG. 2. Collagen fiber alignment quantification. (**A**) SHG microscopy image. (**B**) Fourier transform of image (contrast adjusted). Fourier amplitude components (FFT image intensities) were summed up along angles at 5° increments from 0 to 180° and represented as an arrow and θ. (**C**) Summation of amplitudes resulted in a histogram of the image intensities along each 5° increment; from this histogram the mode was calculated, and the alignment index (AI) was calculated according to Equation 1. SHG, second harmonic generation; FFT, fast fourier transform.

contracted to $75 \pm 2.1\%$ of the original area by day 3 compared with a contraction of $55 \pm 4.1\%$ of the original area for the 2.5 mg/mL annular gels on day 3. The 1 mg/mL disks contracted to $15 \pm 1.1\%$ of original area, whereas 1 mg/mL annular gels contracted to $6.2 \pm 1.4\%$ by day 3. The 1 mg/mL gels contracted very quickly from day 0 to 1 and approached steady state, compared with the slower and more steady contraction seen in the 2.5 mg/mL gels over the 3 days. Neither the disks nor the annular constructs showed a change in thickness over the 3 days of contraction. In addition, constructs showed no difference ($p < 0.05$) between groups in viability after construction with a mean viability of all groups of $92 \pm 2\%$.

Microscale. Collagen distribution inside the constructs changed markedly during the contraction process (Fig. 4A). At day 0, collagen was distributed uniformly throughout the sample. Over the course of 3 days, the distribution became more heterogeneous in the disks, with more collagen evident in the pericellular region surrounding AF cells. This effect occurred at both concentrations, but was more pronounced in 1.0 mg/mL gels. Further, in regions where cells were in tight proximity, collagen fibers were rearranged to form larger bundles on lines between cells (Fig. 4B). On a larger length scale, this collagen rearrangement resulted in the development of circumferential collagen fibril and cellular alignment within the annular gels (Fig. 5).

Fibril orientation

Collagen disks showed little change in fibril alignment over the 3 days of contraction for both the 1 and 2.5 mg/mL disks, as indicated by AI values that ranged from 1.2 to 1.3 over 3 days (data not shown). In contrast to the disk constructs, the annular constructs showed a large degree of fibril alignment in all regions of the constructs over the 3 days of contraction (Fig. 6). The AI of the 1.0 mg/mL annular construct increased from <1.3 at day 0 to 1.6 at day 1, and remained at ~1.6 for day 2 and 3. No significant differences were noticed between regions of the constructs on the same day when the data were analyzed based on region.

In 2.5 mg/mL gels AI increased slowly and more steadily over the 3 days of contraction, changing from ~1.3 on day 1 to 1.4 by day 3 ($p < 0.05$ compared with day 0). In contrast to

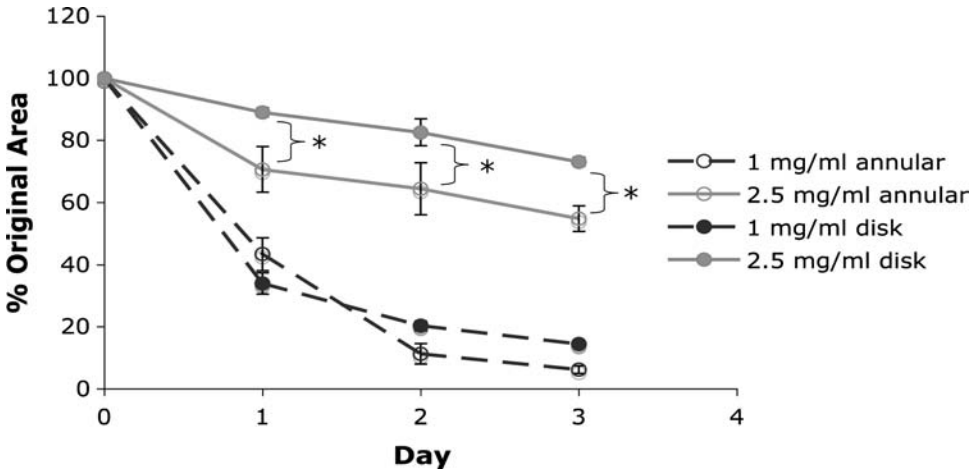

FIG. 3. Contraction of disk and annular gels represented as a percentage of the constructs original surface area. Data presented as means ± standard deviations for $n = 7$ (*$p < 0.05$).

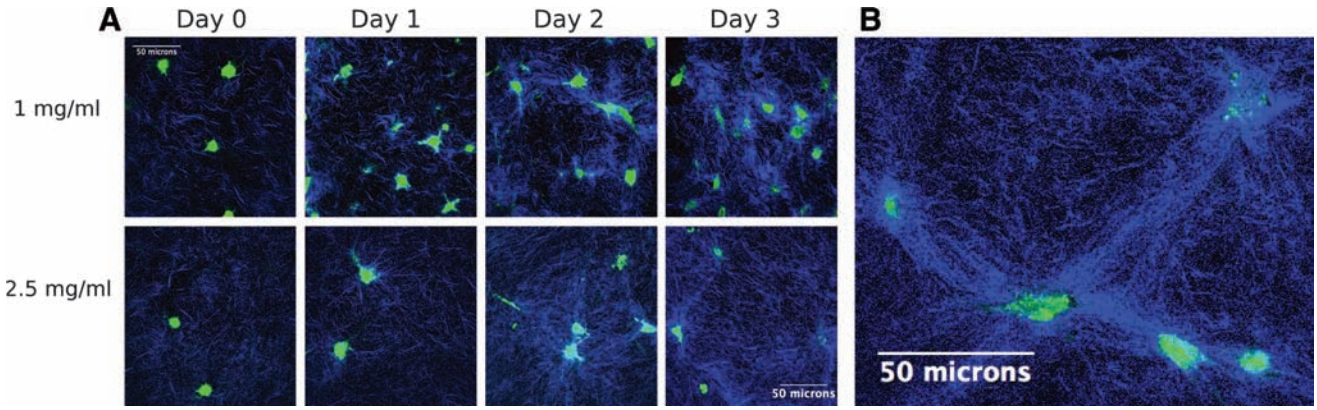

FIG. 4. SHG-TPEF images (**A**) from inside region during contraction of 1 and 2.5 mg/mL collagen disk constructs over 3 days, and (**B**) magnified image showing aligned fibers between cells on day 3 of contraction in 2.5 mg/mL collagen disks (blue, collagen; green, cell). TPEF, two-photon excited fluorescence. Color images available online at www.liebertonline.com/ten.

the 1 mg/mL annular gels, the 2.5 mg/mL gels showed regional heterogeneity, with the middle regions less aligned compared with the inner and outer regions over days 1, 2, and 3 (three-way analysis of variance, $p < 0.05$). The 1 mg/mL gels showed significant increases ($p < 0.05$) in fibril alignment compared with the 2.5 mg/mL gels at day 1, 2, and 3. With time, mode angles progressed toward 90° and distributions became narrower, indicating a direction of alignment in the circumferential direction (Fig. 6C, D). These trends were present for both 1.0 and 2.5 mg/mL gels, but were more pronounced for 1.0 mg/mL gels. Overall, the data indicate a circumferential alignment of collagen fibrils resulting from annular gel contraction around a polyethylene core.

Cellular orientation

Disk gels showed no global alignment of cells over the 3 days of contraction despite showing some evidence of cellular elongation (Fig. 7). However, annular gels showed cellular elongation and circumferential alignment of the cells over the 3 days. The cells developed a spindle-shaped

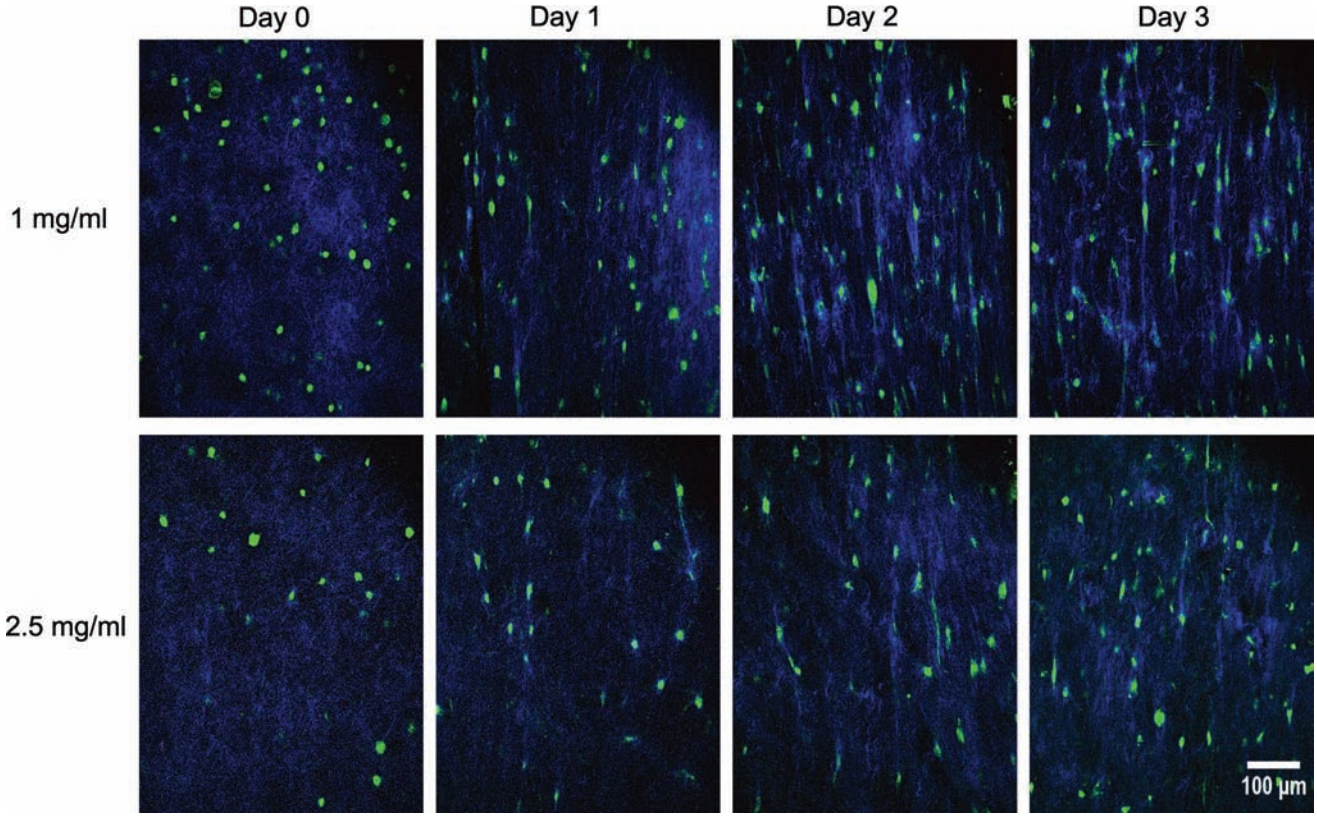

FIG. 5. SHG-TPEF images from inside region during contraction of 1 and 2.5 mg/mL collagen annular constructs over 3 days. Color images available online at www.liebertonline.com/ten.

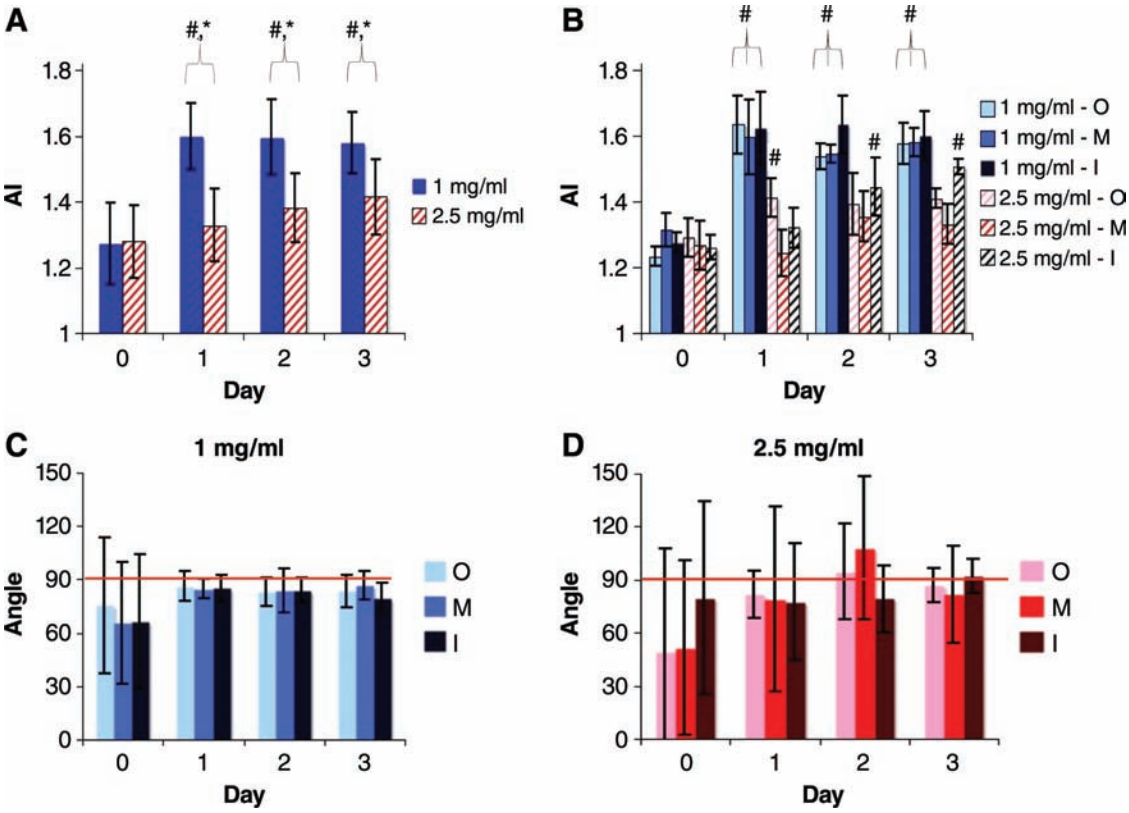

FIG. 6. SHG alignment data for collagen annular gels with (**A**) AI broken down by day and gel concentration ($n = 21$), (**B**) AI further broken down by region of gel ($n = 7$) (O, outside; M, middle; I, inside), and mode angle broken down by day, concentration, and region of gel for (**C**) 1 mg/mL ($n = 4$) and (**D**) 2.5 mg/mL gels ($n = 7$). Data presented as means and standard deviations ($^{\#}p < 0.05$ compared with day 0; $^{*}p < 0.05$ for indicated groups). Color images available online at www.liebertonline.com/ten.

morphology elongated between and parallel to the collagen fibrils similar to the morphology and alignment observed in the IVD.

Composite discs

Composite discs formed in size and shape of rat lumbar IVD. Collagen gel AF analogue seeded with AF cells contracted around alginate NP analog seeded with NP cells. Collagen fibrils produced AI of 1.57 ± 0.06 in the circumferential direction (Fig. 8).

Discussion

The broad goal of this work was to develop a method for self-assembly of an aligned IVD AF construct from seeded collagen gels that can be employed in an engineered IVD composite. This study focuses on remodeling of collagen gels by AF cells and the creation of annular constructs with circumferentially aligned fibrils. Previous efforts to make IVD tissue-engineered constructs have focused mainly on developing the compressive properties of the tissue with less focus on the development of an aligned collagen fibril and cellular architecture in the AF region to provide the necessary tensile and shear properties. Some work has demonstrated the creation of aligned IVD cells in microgrooves[53] and created tissue-engineered scaffolds with aligned nanoscale fiber orientation for use in AF tissue engineering applications.[32,33] However, to date, none of these methods have yielded a composite IVD with aligned collagen fibrils and AF cells around an engineered NP.

In this study, the cellular and fibril architecture were controlled by the boundary conditions imposed on contracting collagen gels. This study demonstrates that over the 3 days of culture, a steady increase of circumferential alignment was observed in both the 2.5 and 1 mg/mL gels (Fig. 7) with a fixed inner boundary. The increased alignment observed in the 1 mg/mL annular gel compared with the 2.5 mg/mL annular gel is likely due to the increased contraction observed in the 1 mg/mL annular gel ($6.2 \pm 1.4\%$ of original area) compared with the 2.5 mg/mL annular gel ($55 \pm 4.1\%$ of original area). The increase in alignment was consistent with the profile of the contraction curves of the two concentrations of gels in the annular gels. Further, similar alignment was observed in a composite construct with a circumferentially aligned collagen AF contracted around an alginate NP (Fig. 8). In contrast to the annular gels and composite, minimal alignment was observed in the disk gels at 3 days. The ability to create an unaligned disk structure in combination with the aligned annular gels may be useful in studying the effects of collagen architecture on tissue development in future studies. Overall, this technique enables control of the degree and heterogeneity of alignment through the original collagen concentrations of the gels and boundary conditions.

Similar techniques have been employed in other tissues to create aligned collagen fibril structures. Costa *et al.*[41] used an

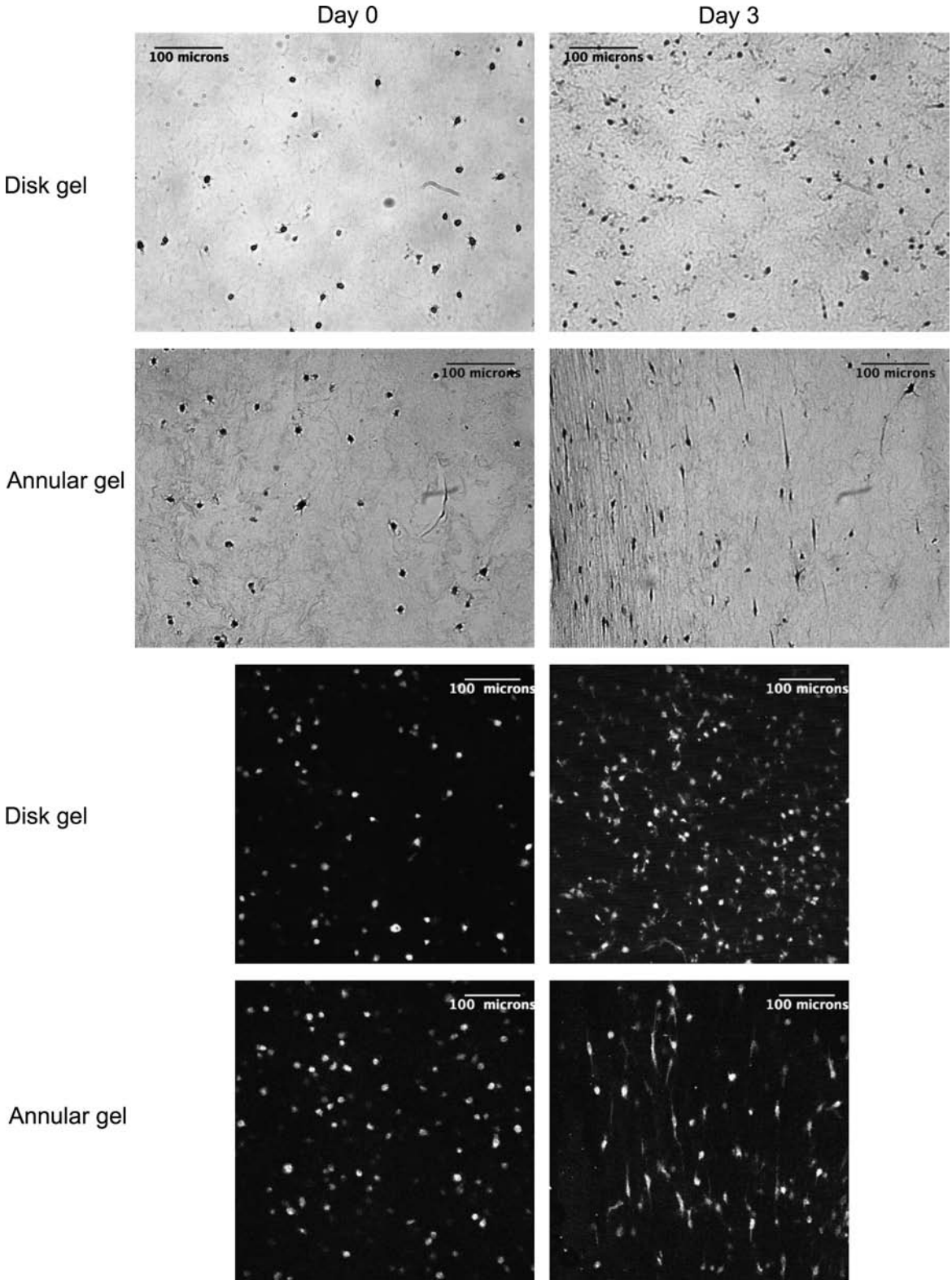

FIG. 7. Hematoxylin and eosin staining and TPEF cellular imaging of 1 mg/mL disk gels and annular gels at day 0 and 3 of contraction from inside region of gel.

analogous technique to create aligned collagen fibrils in engineered heart tissue, whereas Stegemann *et al.*[42] incorporated this technique in engineered blood vessels. Wagenseil *et al.*[54] showed that circumferential alignment developed by fibroblast populated gels resulted in mechanical anisotropy. Schneider *et al.*[55] demonstrated the ability of AF cells to contract collagen/glycosaminoglycan scaffolds. The results of the current study show the ability to use these techniques

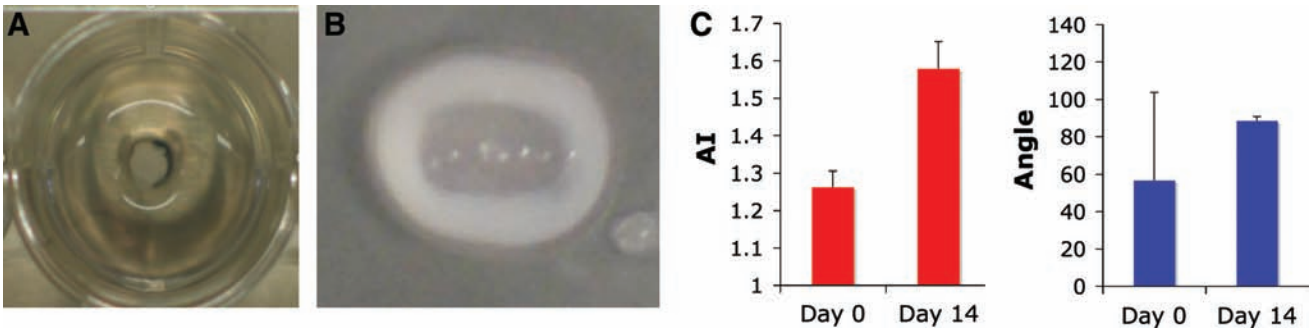

FIG. 8. (**A**) Composite disc before contraction with alginate NP in center of well and collagen solution poured around alginate NP. (**B**) Composite disc after 2 weeks of culture with collagen gel contracted around alginate NP forming tissue-engineered composite intervertebral disc. (**C**) SHG alignment data measured across entirety of contracted collagen gel thickness indicating high degree of collagen alignment in circumferential direction at day 14. NP, nucleus pulposus. Color images available online at www.liebertonline.com/ten.

to create an annular construct with both circumferentially aligned collagen fibrils and aligned AF cells after 3 days of contraction.

Although the main goal of this study was to create collagen alignment in the AF region, it is likely that the cell alignment and shape may be of great importance. To produce a mechanically functional tissue from a collagen gel, long-term culture is likely needed. Fibroblasts are known to increase collagen type I expression when maintained in an aligned spindle shape as compared with a randomly oriented structure and is further enhanced with the application of a tensile stimulation.[56] The spindle-shaped circumferential cellular alignment (Fig. 7) may be advantageous for the future development of the extracellular matrix in long-term culture, as well as for priming AF cells for mechanical stimulation.

The use of SHG-TPEF microscopy enabled the simultaneous study of collagen architecture and cell morphology. More collagen was observed in the pericellular region of the cells in the disk constructs over the 3 days of contraction and was greater in the 1 mg/mL gels than in the 2.5 mg/mL gels. The increased concentration of collagen within these pericellular regions could result from newly synthesized collagen, as suggested by Torkian *et al.*,[57] or from pulling of collagen fibrils into the pericellular region by cells. The observed similar profiles of the gel contraction and the development of the increased pericellular collagen between the two concentrations of gels along with the relatively short culture time suggest a contraction mechanism over a collagen production mechanism. The varying collagen architecture suggests that although tissue-scale variables, such as total collagen concentration, regulate mechanical properties, it is also important to characterize the microscale collagen architecture that may also yield insight into the process of tissue assembly.

The SHG-TPEF images also showed a cell–fibril–cell interaction. As the gels contracted, fibrils were aligned between adjacent cells in the disk and annular gels (Fig. 5). The alignment of collagen networks between two cellular islands seeded in collagen gels has been proposed in model and experimentally observed by Ohsumi *et al.*[58] but can be seen here in the SHG images occurring between individual cells. This provides a possible mechanism for the alignment of fibrils observed within the annular gels. Fibrils first become stretched between the cells; as the cells pull and contract around the fixed inner core, the strained fibrils between cells will be predominately oriented in the circumferential direction due to the imposed physical boundary and circumferential tensile stresses. This would not result in aligned fibrils in unbounded disks as no boundaries have been applied and the cells will contract isotropically. Further, these data suggest the possibility that cell patterning could be employed in collagen gels to further control the resulting collagen architecture of contracted collagen gels in the future.

Despite the advancements presented in this article and observed in the field, the creation of a clinically applicable tissue-engineered IVD faces a number of challenges. One significant challenge is the creation of a disc with sufficient mechanical properties to replace the native IVD. Because mechanical properties are tied to the presence of adequate amounts of collagen and proteoglycan, this requires significant metabolic activity in an environment with low oxygen and high osmolarity.[59,60] In addition to mechanical concerns, an engineered IVD will need to integrate with the native tissue when implanted, and survive in the native disc space environment upon implantation. Despite these challenges the techniques described here for producing an aligned AF represent an important step toward making a functional composite IVD.

Further, collagen alignment in the native AF is not only circumferential in direction, but also at an alternating angle of $\pm 28^{\circ}$ between adjacent lamellae and increasing to 44° at the inner AF.[61,62] Achieving this alternating pattern of alignment remains a persistent challenge in IVD tissue engineering with electrospinning being proposed as a possible solution.[33] However, the current technique enables generation of the dominant circumferential alignment of the collagen fibrils/cells in a composite engineered IVD and provides techniques that in future work may provide this further complexity in structure. Further, the ability to deposit successive layers of collagen gels may enable the generation of constructs with multiple lamellae. As a result, contracting collagen gels provides a powerful tool to create the complex structure of the AF and warrants further investigation.

Disclosure Statement

This work is supported in part by the AO Foundation Research Fund F-08-108 and by the NIH/NIBIB P41 RR04224 to WRZ and RMW. No other competing financial interests exist.

References

1. Ehrlich, G.E. Low back pain. Bull World Health Organ **81,** 671, 2003.
2. Kelsey, J.L., and White, A.A., 3rd. Epidemiology and impact of low-back pain. Spine **5,** 133, 1980.
3. Yasuma, T., Koh, S., Okamura, T., and Yamauchi, Y. Histological changes in aging lumbar intervertebral discs. Their role in protrusions and prolapses. J Bone Joint Surg **72,** 220, 1990.
4. Kuslich, S.D., Ulstrom, C.L., and Michael, C.J. The tissue origin of low back pain and sciatica: a report of pain response to tissue stimulation during operations on the lumbar spine using local anesthesia. Orthop Clin N Am **22,** 181, 1991.
5. O'Neill, C.W., Kurgansky, M.E., Derby, R., and Ryan, D.P. Disc stimulation and patterns of referred pain. Spine **27,** 2776, 2002.
6. Eyre, D.R. Biochemistry of the intervertebral disc. Int Rev Connect Tissue Res **8,** 227, 1979.
7. Bruehlmann, S.B., Rattner, J.B., Matyas, J.R., and Duncan, N.A. Regional variations in the cellular matrix of the annulus fibrosus of the intervertebral disc. J Anat **201,** 159, 2002.
8. Baer, A.E., Laursen, T.A., Guilak, F., and Setton, L.A. The micromechanical environment of intervertebral disc cells determined by a finite deformation, anisotropic, and biphasic finite element model. J Biomech Eng **125,** 1, 2003.
9. Maldonado, B.A., and Oegema, T.R., Jr. Initial characterization of the metabolism of intervertebral disc cells encapsulated in microspheres. J Orthop Res **10,** 677, 1992.
10. Broberg, K.B. On the mechanical behaviour of intervertebral discs. Spine **8,** 151, 1983.
11. Schollmeier, G., Lahr-Eigen, R., and Lewandrowski, K.U. Observations on fiber-forming collagens in the anulus fibrosus. Spine **25,** 2736, 2000.
12. Nerlich, A.G., Boos, N., Wiest, I., and Aebi, M. Immunolocalization of major interstitial collagen types in human lumbar intervertebral discs of various ages. Virchows Arch **432,** 67, 1998.
13. Beard, H.K., Roberts, S., and O'Brien, J.P. Immunofluorescent staining for collagen and proteoglycan in normal and scoliotic intervertebral discs. J Bone Joint Surg **63B,** 529, 1981.
14. Beard, H.K., Ryvar, R., Brown, R., and Muir, H. Immunochemical localization of collagen types and proteoglycan in pig intervertebral discs. Immunology **41,** 491, 1980.
15. Adams, P., Eyre, D.R., and Muir, H. Biochemical aspects of development and ageing of human lumbar intervertebral discs. Rheumatol Rehabil **16,** 22, 1977.
16. Eyre, D.R., and Muir, H. Types I and II collagens in intervertebral disc. Interchanging radial distributions in annulus fibrosus. Biochem J **157,** 267, 1976.
17. Guerin, H.L., and Elliott, D.M. Quantifying the contributions of structure to annulus fibrosus mechanical function using a nonlinear, anisotropic, hyperelastic model. J Orthop Res **25,** 508, 2007.
18. Diwan, A.D., Parvataneni, H.K., Khan, S.N., Sandhu, H.S., Girardi, F.P., and Cammisa, F.P., Jr. Current concepts in intervertebral disc restoration. Orthop Clin N Am **31,** 453, 2000.
19. Huang, R.C., and Sandhu, H.S. The current status of lumbar total disc replacement. Orthop Clin N Am **35,** 33, 2004.
20. Guyer, R.D., McAfee, P.C., Hochschuler, S.H., Blumenthal, S.L., Fedder, I.L., Ohnmeiss, D.D., and Cunningham, B.W. Prospective randomized study of the Charite artificial disc: data from two investigational centers. Spine J **4,** 252S, 2004.
21. Bertagnoli, R., Yue, J.J., Pfeiffer, F., Fenk-Mayer, A., Lawrence, J.P., Kershaw, T., and Nanieva, R. Early results after ProDisc-C cervical disc replacement. J Neurosurg **2,** 403, 2005.
22. Blumenthal, S., McAfee, P.C., Guyer, R.D., Hochschuler, S.H., Geisler, F.H., Holt, R.T., Garcia, R., Jr., Regan, J.J., and Ohnmeiss, D.D. A prospective, randomized, multicenter Food and Drug Administration investigational device exemptions study of lumbar total disc replacement with the CHARITE artificial disc versus lumbar fusion: part I: evaluation of clinical outcomes. Spine **30,** 1565, 2005.
23. McAfee, P.C., Cunningham, B., Holsapple, G., Adams, K., Blumenthal, S., Guyer, R.D., Dmietriev, A., Maxwell, J.H., Regan, J.J., and Isaza, J. A prospective, randomized, multicenter Food and Drug Administration investigational device exemption study of lumbar total disc replacement with the CHARITE artificial disc versus lumbar fusion: part II: evaluation of radiographic outcomes and correlation of surgical technique accuracy with clinical outcomes. Spine **30,** 1576, 2005.
24. Sun, Y., Hurtig, M., Pilliar, R.M., Grynpas, M., and Kandel, R.A. Characterization of nucleus pulposus-like tissue formed *in vitro*. J Orthop Res **19,** 1078, 2001.
25. Ganey, T., Libera, J., Moos, V., Alasevic, O., Fritsch, K.G., Meisel, H.J., and Hutton, W.C. Disc chondrocyte transplantation in a canine model: a treatment for degenerated or damaged intervertebral disc. Spine **28,** 2609, 2003.
26. Watanabe, K., Mochida, J., Nomura, T., Okuma, M., Sakabe, K., and Seiki, K. Effect of reinsertion of activated nucleus pulposus on disc degeneration: an experimental study on various types of collagen in degenerative discs. Connect Tissue Res **44,** 104, 2003.
27. Gorensek, M., Jaksimovic, C., Kregar-Velikonja, N., Gorensek, M., Knezevic, M., Jeras, M., Pavlovcic, V., and Cor, A. Nucleus pulposus repair with cultured autologous elastic cartilage derived chondrocytes. Cell Mol Biol Lett **9,** 363, 2004.
28. Seguin, C.A., Grynpas, M.D., Pilliar, R.M., Waldman, S.D., and Kandel, R.A. Tissue engineered nucleus pulposus tissue formed on a porous calcium polyphosphate substrate. Spine **29,** 1299, 2004.
29. Chang, G., Kim, H.J., Kaplan, D., Vunjak-Novakovic, G., and Kandel, R.A. Porous silk scaffolds can be used for tissue engineering annulus fibrosus. Eur Spine J **16,** 1848, 2007.
30. Shao, X., and Hunter, C.J. Developing an alginate/chitosan hybrid fiber scaffold for annulus fibrosus cells. J Biomed Mater Res **82,** 701, 2007.
31. Wan, Y., Feng, G., Shen, F.H., Laurencin, C.T., and Li, X. Biphasic scaffold for annulus fibrosus tissue regeneration. Biomaterials **29,** 643, 2008.
32. Nerurkar, N.L., Elliott, D.M., and Mauck, R.L. Mechanics of oriented electrospun nanofibrous scaffolds for annulus fibrosus tissue engineering. J Orthop Res **25,** 1018, 2007.
33. Nerurkar, N.L., Mauck, R.L., and Elliott, D.M. ISSLS prize winner: integrating theoretical and experimental methods for functional tissue engineering of the annulus fibrosus. Spine **33,** 2691, 2008.
34. Nesti, L.J., Li, W.J., Shanti, R.M., Jiang, Y.J., Jackson, W., Freedman, B.A., Kuklo, T.R., Giuliani, J.R., and Tuan, R.S. Intervertebral disc tissue engineering using a novel hyaluronic acid-nanofibrous scaffold (HANFS) amalgam. Tissue Eng **14,** 1527, 2008.

35. Saad, L., and Spector, M. Effects of collagen type on the behavior of adult canine annulus fibrosus cells in collagen-glycosaminoglycan scaffolds. J Biomed Mater Res **71,** 233, 2004.
36. Mizuno, H., Roy, A.K., Vacanti, C.A., Kojima, K., Ueda, M., and Bonassar, L.J. Tissue-engineered composites of anulus fibrosus and nucleus pulposus for intervertebral disc replacement. Spine **29,** 1290, 2004.
37. Mizuno, H., Roy, A.K., Zaporojan, V., Vacanti, C.A., Ueda, M., and Bonassar, L.J. Biomechanical and biochemical characterization of composite tissue-engineered intervertebral discs. Biomaterials **27,** 362, 2006.
38. Barocas, V.H., Girton, T.S., and Tranquillo, R.T. Engineered alignment in media equivalents: magnetic prealignment and mandrel compaction. J Biomech Eng **120,** 660, 1998.
39. Grinnell, F., and Lamke, C.R. Reorganization of hydrated collagen lattices by human skin fibroblasts. J Cell Sci **66,** 51, 1984.
40. Thomopoulos, S., Fomovsky, G.M., and Holmes, J.W. The development of structural and mechanical anisotropy in fibroblast populated collagen gels. J Biomech Eng **127,** 742, 2005.
41. Costa, K.D., Lee, E.J., and Holmes, J.W. Creating alignment and anisotropy in engineered heart tissue: role of boundary conditions in a model three-dimensional culture system. Tissue Eng **9,** 567, 2003.
42. Stegemann, J.P., Dey, N.B., Lincoln, T.M., and Nerem, R.M. Genetic modification of smooth muscle cells to control phenotype and function in vascular tissue engineering. Tissue Eng **10,** 189, 2004.
43. Zoumi, A., Yeh, A., and Tromberg, B.J. Imaging cells and extracellular matrix *in vivo* by using second-harmonic generation and two-photon excited fluorescence. Proc Natl Acad Sci USA **99,** 11014, 2002.
44. Williams, R.M., Zipfel, W.R., and Webb, W.W. Interpreting second-harmonic generation images of collagen I fibrils. Biophys J **88,** 1377, 2005.
45. Zipfel, W.R., Williams, R.M., Christie, R., Nikitin, A.Y., Hyman, B.T., and Webb, W.W. Live tissue intrinsic emission microscopy using multiphoton-excited native fluorescence and second harmonic generation. Proc Natl Acad Sci USA **100,** 7075, 2003.
46. Elsdale, T., and Bard, J. Collagen substrata for studies on cell behavior. J Cell Biol **54,** 626, 1972.
47. Saltzman, W.M., Parkhurst, M.R., Parsons-Wingerter, P., and Zhu, W.H. Three-dimensional cell cultures mimic tissues. Ann NY Acad Sci **665,** 259, 1992.
48. Ng, C.P., Hinz, B., and Swartz, M.A. Interstitial fluid flow induces myofibroblast differentiation and collagen alignment *in vitro*. J Cell Sci **118,** 4731, 2005.
49. Chaudhuri, S., Nguyen, H., Rangayyan, R.M., Walsh, S., and Frank, C.B. A fourier domain directional filtering method for analysis of collagen alignment in ligaments. IEEE Trans biomed Eng **34,** 509, 1987.
50. Pourdeyhimi, B., Dent, R., and Davis, H. Measuring fiber orientation in nonwovens: 3. Fourier transform. Textile Res J **67,** 143, 1997.
51. Nishimura, T., and Ansell, M.P. Fast fourier transform and filtered image analyses of fiber orientation in OSB. Wood Sci Technol **36,** 287, 2002.
52. van Zuijlen, P.P., de Vries, H.J., Lamme, E.N., Coppens, J.E., van Marle, J., Kreis, R.W., and Middelkoop, E. Morphometry of dermal collagen orientation by fourier analysis is superior to multi-observer assessment. J Pathol **198,** 284, 2002.
53. Johnson, W.E., Wootton, A., El Haj, A., Eisenstein, S.M., Curtis, A.S., and Roberts, S. Topographical guidance of intervertebral disc cell growth *in vitro*: towards the development of tissue repair strategies for the anulus fibrosus. Eur Spine J **15 Suppl 3,** S389, 2006.
54. Wagenseil, J.E., Elson, E.L., and Okamoto, R.J. Cell orientation influences the biaxial mechanical properties of fibroblast populated collagen vessels. Ann Biomed Eng **32,** 720, 2004.
55. Schneider, T.O., Mueller, S.M., Shortkroff, S., and Spector, M. Expression of alpha-smooth muscle actin in canine intervertebral disc cells *in situ* and in collagen-glycosaminoglycan matrices *in vitro*. J Orthop Res **17,** 192, 1999.
56. Lee, C.H., Shin, H.J., Cho, I.H., Kang, Y.M., Kim, I.A., Park, K.D., and Shin, J.W. Nanofiber alignment and direction of mechanical strain affect the ECM production of human ACL fibroblast. Biomaterials **26,** 1261, 2005.
57. Torkian, B.A., Yeh, A.T., Engel, R., Sun, C.H., Tromberg, B.J., and Wong, B.J. Modeling aberrant wound healing using tissue-engineered skin constructs and multiphoton microscopy. Arch Facial Plast Surg **6,** 180, 2004.
58. Ohsumi, T.K., Flaherty, J.E., Evans, M.C., and Barocas, V.H. Three-dimensional simulation of anisotropic cell-driven collagen gel compaction. Biomech Model Mechanobiol **7,** 53, 2007.
59. Kobayashi, S., Meir, A., and Urban, J. Effect of cell density on the rate of glycosaminoglycan accumulation by disc and cartilage cells *in vitro*. J Orthop Res **26,** 493, 2008.
60. Grunhagen, T., Wilde, G., Soukane, D.M., Shirazi-Adl, S.A., and Urban, J.P. Nutrient supply and intervertebral disc metabolism. J Bone Joint Surg Am 88 Suppl **2,** 30, 2006.
61. Cassidy, J.J., Hiltner, A., and Baer, E. Hierarchical structure of the intervertebral disc. Connect Tissue Res **23,** 75, 1989.
62. Marchand, F., and Ahmed, A.M. Investigation of the laminate structure of lumbar disc anulus fibrosus. Spine **15,** 402, 1990.

Address correspondence to:
Lawrence J. Bonassar, Ph.D.
Department of Biomedical Engineering & Sibley School of Mechanical and Aerospace Engineering
Cornell University
149 Weill Hall
Ithaca, NY 14853

E-mail: lb244@cornell.edu

Received: June 30, 2009
Accepted: November 10, 2009
Online Publication Date: January 6, 2010